Contour Optimization of a Pin Insulator Using Neural Network

Fidelis Aimua

Submitted to the
Institute of Graduate Studies and Research
in partial fulfillment of the requirements for the Degree of

Master of Science
in
Electrical and Electronic Engineering

Eastern Mediterranean University
February 2015
Gazimağusa, North Cyprus

Approval of the Institute of Graduate Studies and Research

Prof. Dr. Serhan Çiftçioğlu
Acting Director

I certify that this thesis satisfies the requirements as a thesis for the degree of Master of Science in Electrical and Electronic Engineering.

Prof. Dr. Hasan Demirel
Chair, Department of Electrical and Electronic Engineering

We certify that we have read this thesis and that in our opinion it is fully adequate in scope and quality as a thesis for the degree of Master of Science in Electrical Electronic Engineering.

Asst. Prof. Dr. Suna Bolat
Supervisor

Examining Committee

1. Prof. Dr. Osman Kükrer. _____

2. Prof. Dr. Hüseyin Özkaramanlı _____

3. Asst. Prof. Dr. Suna Bolat _____

ABSTRACT

Insulator geometry strongly affects the distribution of electric field along the surface of the insulator. If the field distribution is not uniform, that stresses the insulator unevenly which most often may lead to unnecessary loss of energy, flashover and eventual breakdown of the power network system. As the desire to have a more efficient, effective and reliable system devoid of losses increases; the need for a well optimized insulator arises.

In this study, neural network is used to obtain an optimized form of a pin insulator. Neural network is trained by using geometric information of the pin insulator and field intensities in order to provide a field distribution as uniform and minimum as possible along the insulator surface. Electric field intensities along the surface for different insulator profiles are obtained numerically by using finite element method.

Finally, the result obtained such as the mean absolute error of less than 0.1 at optimum, shows that the network has successfully been used to optimize the contour geometry of the pin insulator.

Keywords: High voltage, insulator, contour optimization, neural network, electric field distribution.

ÖZ

İzolatör geometirisi, izolator yüzeyindeki elektrik alan dağılımını büyük oranda etkiler. Eğer izolatör yüzeyinde elektrik alan dağılımı düzgün değilse, izolatör zorlanır; bu durum genellikle güç sisteminde gereksiz enerji kaybına, atlamaya ve zamanla delinmeye yol açabilir. Daha verimli, etkin ve güvenilir kayıpsız bir sistem ihtiyacı arttıkça, optimum izolatör ihtiyacı da artar.

Bu çalışmada, bir mesnet izolatörünün optimizasyonu için yapay sinir apı kullanılmıştır. Yapay sinir ağı, izolatörün geometrik bilgileri ve alan şiddetleri kullanılarak mümkün oladuğu kadar düzgün ve düşük şiddetli alan dağılımı sağlayacak şekilde eğitilmiştir. Farklı izolatör biçimleri için yüzey boyunca elektrik alan şiddetleri, sonlu elemanlar yöntemi kullanılarak sayısal olarak elde edilmiştir.

Elde edilen sonuç, % 0,1 ortalama mutlak hata ile, sinir ağının mesnet izolatörü optimizasyonunda başarılı olduğunu göstermektedir.

Anahtar Kelimeler: Yüksek gerilim, izolatör, biçim optimizasyonu, yapay sinir ağı, elektrik alan dağılımı.

Dedicated to the one that died and resurrected (JESUS), to my mum Mrs GET Aimua and the memory of my late father (Peter Idahose Alexandre Aimua)

ACKNOWLEDGMENT

Special thanks to my ever hardworking supervisor, Asst. Prof. Dr. Suna Bolat for being such an inspiration to me not just only during this research work but also throughout my studies here.

I also wish to extend my profound gratitude to other members of staff of the faculty of Engineering and Technology, Eastern Mediterranean University.

My hommies are not left out (Ogbole Collins, Cyril Ede, Nnaemeka, Miriam, Ehi Ogbeba) you guys rock and were like a family from home.

Finally, my utmost gratitude goes to my family (Peter Idahose Alexandre Aimua) for your support and prayers with special thanks to Andrew O. Aimua for your brotherly role. You are truly a definition of a “brother”.

TABLE OF CONTENTS

LIST OF TABLES

LIST OF FIGURES

LIST OF ABBREVIATIONS

MAE:	Mean Absolute Error
RMSE:	Root Mean Square Error
ANN:	Artificial Neural Network
MSE:	Mean Squared Error
$\boldsymbol{\mu}$:	Momentum constant
η:	Learning rate

Chapter 1

INTRODUCTION

1.1 Problem Statement

For an effective and efficient delivery of electrical energy particularly in high voltage system, it is of great importance to ensure that the insulation system is resistant to system failures under normal operations. Constant breakdown and continuous degradation of insulation has been a major cause for reduction in power system efficiency [1], continuous increase in power losses and constant outages as experienced over the years have also been attributed to poor insulation mechanism. Furthermore, the cost implications incurred either in the installation process, design or maintenance has since been linked to poor design of insulators; thus a need for the study of insulator contours is of great importance.

Distribution of electric field along insulator surfaces is usually affected by the geometry [2]. From [2], it is noted that flashover do occur along the insulator surface, if the tangential components of its potential gradient exceeds a critical level to sustain discharge, thus this may lead to a total breakdown of the system. In order to arrest such breakdown, the insulator contour should be designed in such a way as to obtain a desired uniform stress and have a minimal tangential electric field.

For the purpose of this research work, an Artificial Neural Network is applied to obtain optimum contour pin type insulator to provide uniform stress distribution

along the surface. Electric field intensities along the surface, average and maximum electric field at the surface of the insulator are calculated for different insulator profiles by finite element method which would serve as an input data for the network. Geometric information of the insulator acts as the output of the network. Using these data, an optimized insulator contour can be determined to have a field distribution as uniform and minimum as possible.

1.2 Thesis objective

1. To understand the essence of using insulators in high voltage transmission.
2. To understand the working mechanism of Artificial Neural Network
3. To obtain an optimized insulator contour geometry that gives uniform stress distribution while keeping the electric field along its surface as minimum as possible.

1.3 Thesis outline

This thesis has been divided into six different chapters.

The first chapter deals on the aim, its objectives and introduces the research work. It presents the problem statement which give rise to the need for this work.

The second chapter takes on the literature of previous works carried out by other researchers using Artificial Neural Network both in high voltage fields and other fields. The electric stress and the factors that affect its distribution in an insulator are discussed. Finally, the finite element method as a numerical method of calculating electric field is analyzed.

Chapter 3 deals entirely on artificial neural network, and its learning pattern.

In chapter four, the methodology of the work is discussed. It gives a vivid description of how numerical method was applied in obtaining the electric field needed in the training of the network, the finite element software applied and an in-depth description of the architecture and the training process involved in the Artificial Neural Network Model.

The results and discussion is contained in Chapter 5 while the 6th and final Chapter contains the thesis conclusion and a recommendation for future work.

Chapter 2

LITERATURE REVIEW

2.1 Overview

In a bid to optimize insulator and electrode contours with complex geometry, different researchers have tried to apply different techniques to achieve this feat. In [3], corona onset was applied in its optimization process. In this work, the corona onset voltage measured was compared with surface electric field as its optimization criterion. It was discovered that its corona onset can result in a modest but measurable increase in corona onset voltage.

In 2002 [4], a 35 kV vacuum interrupter was optimized using the Tabu Search Algorithm. It applied the finite element method in the computation of the electric field which was used in the process. The continuous needs for an optimized insulator use in power system continue to get serious attention owing to its major importance in power system delivery.

K. Kato et al., in his work [5] tried to design an electrode contour with best insulation performance on the basis of area and volume effect in the breakdown field strength. They considered the breakdown characteristics instead of the electric field distribution. In their work, he found out that using the breakdown strength with consideration of its volume and area considerably improved the breakdown voltage as compared to using electric field.

Smoothing cubic splines has also been applied for the same purpose [6]. Local field derivatives were used to determine the necessary displacement to achieve predefined field strength intensity at each point. This he did iteratively in case of failure is step one while applying the smoothing cubic splines in controlling the contour geometry. The effects of contact angle, radius of curvature and the type of material on the electric field has also been considered [7], here the electric field is calculated using the charge simulation method technique at the triple junction as its junction geometry function. He varied the field dependence in accordance with the different variations of contact angle and discovered that electric field varies with angles. The dynamically adjustable algorithm was used for the optimization of a suspension insulator [2]. His aim was to minimize and make the tangential electric field uniform and reduce the insulator size.

As the geometry of the various models of insulator became more complex and a need for an optimized form, either to minimize cost, or to have an optimal performance, various researchers have turned to using the Artificial Neural Network in achieving this feat. For instance, in [8] neural network was used to optimize the contour of axi-symmetrical insulator in a multi-dielectric arrangement. He employed the multilayer feed-forward network with error back propagation and with resilient propagation learning algorithm. S. Charkravorti et al., [9] in 1994 demonstrated the effectiveness of neural network in electric field problems by applying a simple cylindrical electrode system. In his findings, he found out that neural network could give an accuracy of a mean absolute error of about 3%. Neural network has not only been successful in power system but has also had wide use even in weather predictions as seen in [10]. In 2008, daily global solar radiation was predicted by developing a

model with the help of neural network [11]. Furthermore, neural network applications extend even to disaster prediction as it has been successfully used in earthquake prediction [12]. Security application cannot be left out as well. In the area of control system, its application has adequately been deployed as it was used in capacitor control system [13].

Most insulator designers have a single motive, which is to ensure that the insulator has a minimal but uniformly distributed electric field along its surface. For this thesis work, the insulator to be optimized is the porcelain pin insulator. However, one has to understand the concept of electric field stress, trying to have it uniformly distributed by subjecting the pin geometry to finite element method so as to obtain the electric field needed for the optimization process.

Thus in this work, the neural network is applied in optimizing the pin insulator geometry. This is due to its versatility in analyzing complex geometry.

2.2 Porcelain Pin Insulator

The porcelain pin insulators are widely used in voltage transmission of up to 33 kV. Owing to its bulky nature, it becomes highly uneconomical if deployed for use for higher voltage. However, despite this singular limitation observed, its advantages are enormous. Such of those examples include zero porosity, high dielectric resistance, and high mechanical resistance, chemically inert and high outdoor resistance amongst others. Figure 2.1 shows a typical pin porcelain insulator.

Figure 2.1: A Pin insulator

2.3 Electric Field Stress

In-order to design an insulator with optimum performance, it is necessary to grasp the electric field strength experienced particularly with high-level voltage transmission. The stress on dielectric by electric field is known as the electric stress. The magnitude of the field stress on the dielectric is measured using its field intensity. Electric field strength is termed as the electrostatic force per unit positive test charge positioned at a particular point in a dielectric. It is represented with the symbol ‘E’ and its unit is ‘Newton per Coulomb’. In Figure 2.2 a typical illustration of an electric field is shown.

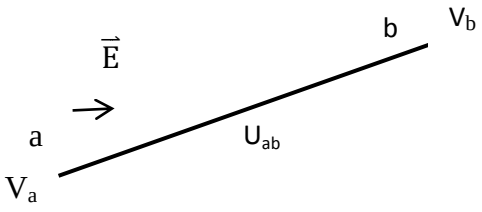

Figure 2.2: Electric field between a and b

In Figure 2.2, the potential difference U_{ab} having V_A and V_b as its potentials in an electric field $\vec{E}$ is described as work done in moving a one positive charge from point b to point a by an external force. Thus,

$$U_{ab} = -\int_b^a |\vec{E}|\, dx = (V_a - V_b) \tag{2.1}$$

The maximum electric field is experienced when the direction of increment in the potential is mostly opposite the path of $\vec{E}$,

$$\frac{dU_{ab}}{dx}\Big|_{max} = -|\vec{E}|_{max} \tag{2.2}$$

From equation (2.2), a physical interpretation of the process of finding electric field intensity from the scalar potential 'V' is obtained. The operator on V by which $\vec{E}$ is obtained is thus known as the gradient. Therefore the relationship between V and $\vec{E}$ is given as

$$\vec{E} = -\nabla V \tag{2.3}$$

where;

$\vec{E}$: Electric field

V: scalar potential

Equation (2.3) is referred to as gradient of the electric field potential.

2.4 Parameters Affecting Electric Stress Distribution In Insulators

2.4.1 Shape of insulator

This plays a significant role in determining the electric field stress distribution in an insulator. To ensure that the insulator is of good design, it must have an electric field stress below its ionization threshold. Researches have shown that the electric field strength tends to be higher along the sheds than in adjacent areas of the insulator. Owing to its rounding curvature, it tends to attract more stress and as such needs to

be well optimized to obtain a uniformly distributed stress and minimize the field strength experienced around it.

2.4.2 Permittivity of the material

This determines how much electric field or flux is generated per unit charge. A medium with higher permittivity is likely to have less flux owing to its polarization. It is related directly to electric susceptibility. Kaana-Nkusi et al. [14] in his work calculated the voltage and electric field distribution along a post insulator. He considered a number of different criteria such as the electric flux density, potential error and tangential field strength. His findings showed that higher dielectric permittivity of an insulator correspond to an increment in value of electric field along the surface. Relative permittivity of some materials include, porcelain is 5-7, air is1, water between 4 and 8.

2.4.3 Potential difference

The electric field stress is affected by the potential difference across it. A measure of force per unit charge is the electric field and the energy per unit charge is the potential energy. Now if we assume that a unit test charge is to be moved from x to y, its work done which is the electric potential is related to the electric field with the equation (2.4)

$$\vec{E} = -\frac{\Delta V}{\Delta d} \tag{2.4}$$

where;

$\vec{E}$: electric field

ΔV: potential difference

Δd: distance moved between x and y

$(-)$ sign shows that the potential decreases as it moves in the direction of the field.

2.4.4 External factors

Adverse environmental conditions affect high voltage insulators since they are deployed for outside use. Some of these conditions include rain, fog, and dew, industrial as well as agricultural pollution. They stick to the surface of the insulators and in most cases are dormant. It gets activated once the air becomes humid. A conductive film is formed leading to an increase in the conductance of the insulator thereby increasing the leakage current, reducing its flashover voltage. Researches have shown that, contamination on the surface of insulator, affects the electric field greatly [15].

2.5 Electric Field Analysis Using Numerical Method.

There are different numerical methods known for electric field calculation. They include, charge simulation method, boundary element method, finite difference method and the finite element method. However, for this thesis, the finite element method is used thus discussion would be limited to this method.

2.5.1 Finite Element Method

This is one of the most commonly used methods by engineers in calculating electric field. Its principles lie on transforming differential equation in integral structure and approximating it. The easiest way in transforming this is finding an operation that abates the energy in whole. Thus its calculations can easily be achieved if one calculates the electric potential distribution first and then the field distribution by deducting the gradient of electric potential from it.

From Maxwell equation,

$$\nabla . \vec{E} = \frac{\rho}{\varepsilon} \tag{2.5}$$

where;

ρ: the volume charge density

ε: permittivity of the dielectric material ($\varepsilon = \varepsilon_o\varepsilon_r$)

ε_o: permittivity of air (8.854×10^{-14})

ε_r: permittivity of the dielectric material.

From equation (2.3) and (2.5), the Poisson equation is obtained by substituting (2.5) into (2.3);

$$\nabla^2 V = -\frac{\rho}{\varepsilon} \tag{2.6}$$

The Laplace equation is obtained when the space charge $\rho = 0$ and equation (2.6) becomes

$$\nabla^2 V = 0 \tag{2.7}$$

But for a finite element method, its basic approach for obtaining the electric field involves that for electrostatic, the entire energy acquires a minutest quantity in the whole field. Thus, the potential V under given conditions should make the enclosed energy function to be given at a minimum for a given dielectric volume 'υ'

Thus;

$$W = \int_{\upsilon} \frac{1}{2} \varepsilon (\nabla V)^2 d\upsilon \tag{2.8}$$

where

υ: dielectric volume under consideration

W: electrical energy stored in the volume of dielectric in view and is obtained by computing the simple equation in (2.3)

Using this process, field between electrodes being considered is split into fixed quantity of distinct elements. Nodes and elements are allotted specific integer

numbers. The distinct element silhouette is chosen as triangular for a 2-dimensional or tetrahedral for a 3-dimensional. This is illustrated in figure 2.3 and figure 2.4. At locations were higher field intensity is present, discrete elements of minute size covers it.

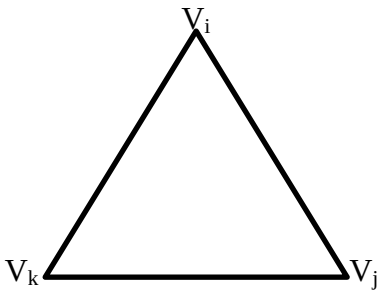

Figure 2.3: Triangular

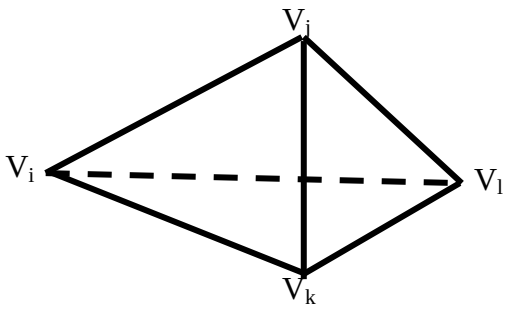

Figure 2.4: Tetrahedral

From equation (2.8), if the electrostatic field is not distorted by any space charge, potential will be determined by boundaries. Thus equation (2.8) becomes

$$W = \iiint_{\upsilon} \left[\frac{1}{2}\,\varepsilon\left\{\left(\frac{\partial V}{\partial x}\right)^2 + \left(\frac{\partial V}{\partial y}\right)^2 + \left(\frac{\partial V}{\partial z}\right)^2\right\}\right] dxdydz \qquad (2.9)$$

Equation (2.9) is for the Cartesian coordinate.

For a small volume element $d\upsilon = (dx\ dy\ dz)$ and the expression $(1/2\ \varepsilon\ \Delta^2 V)$ within equation (2.9) represent the energy densities per unit volume in a given direction.

In the case of two dimensions, it is assumed that potential distribution does not change in the z direction, thus total energy W_A stored within area A can be given by equation (2.8)

$$W_A = \int_A \frac{1}{2}\varepsilon(\nabla V)^2 dA$$

And from equation (2.9), in this case

$$W = z \iint_A \left[\frac{1}{2}\varepsilon\left\{\left(\frac{\partial V}{\partial x}\right)^2 + \left(\frac{\partial V}{\partial y}\right)^2\right\}\right] dxdy \qquad (2.10)$$

where z is a constant. Inside each sub-domain, a linear dependency of V on x and y is assumed and gives rise to the first order approximation,

$$V(x,y) = V = a_{e1} + a_{e2}x + a_{e3}y \qquad (2.11)$$

where V is the electrical potential of any arbitrary point inside each sub-domain, a_{e1},a_{e2},a_{e3}, are the computational coefficient for a triangle element e. Thus equation (2.11) implies that within the element, the potential are linearly distributed and field intensity constant.

In order to minimize the energy within the field region under consideration, only derivatives of the energies with respect to the potential distribution in each element are of particular interest. For the element under consideration, W_e is the energy enclosed within the element, then the energy per unit length denoted here by $W_{\Delta e}$ can be given as follows,

$$W_{\Delta e} = \frac{1}{2}\Delta_e \varepsilon\left[\left(\frac{\partial V}{\partial x}\right)^2 + \left(\frac{\partial V}{\partial y}\right)^2\right] \qquad (2.12)$$

Symbol Δ_e represents the area of the discrete triangular element under consideration. If the total energy in the whole field of given element is denoted by W_Δ, the relation for minimizing the energy within the entire can be given as

$$\frac{\partial W_\Delta}{\partial [V]} = 0 \tag{2.13}$$

where [V] is the total potential vector for all the nodes within a given system.

Chapter 3

ARTIFICIAL NEURAL NETWORK

3.1 Introduction

An artificial neural network is massively parallel system relying on dense management of interconnections and surprisingly, simple processors. Its simple processing units have the tendency of storing experimental data and make it available for us when required. In [16], it relates it behavior to that of human because of its ability to mimic the brain. They are not programmed but learn by example [16]. It can also be described as a set of neurons connected in biologically arranged format in form of layers. Figure 3.1 depicts the structure of a feed-forward network. The neuron number in each of the layer is represented by N_i , In the i^{th} layer and the inputs served to these neurons are linked to the neurons in the preceding layer. The signal that excites system is received by the input layer. Each neuron has a weight attached to it and the training of artificial neural network practically deals with adjustment of this weights. The learning of this network relies on the input given to it, thus sets of data tagged as training data is needed for its training.

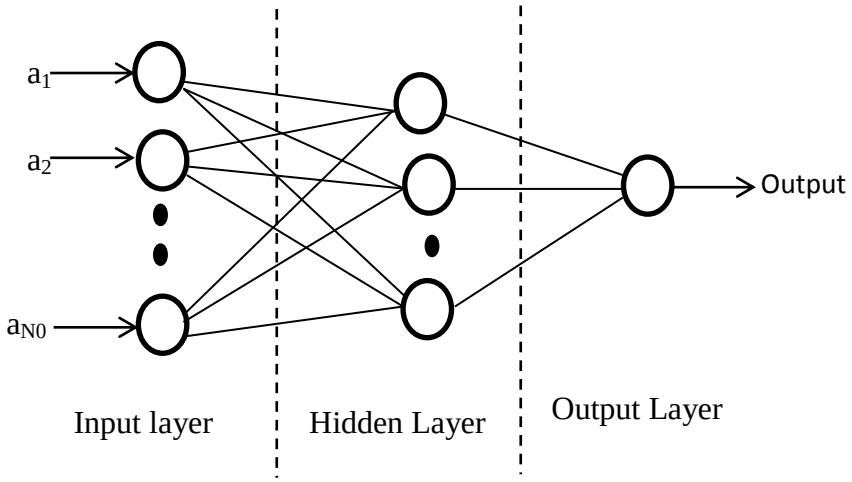

Figure 3.1: A three layer ANN feedforward architecture

In Figure 3.1, the inputs to the network are $a_1, a_2 \ldots . a_{N0.}$ Owing to its high level performance in pattern recognition, artificial neural network are deployed to use in different fields including signal processing. Despite its wide applications, some draw backs still exist in it. Out of these draw backs is the lack of a guiding principle in choosing the actual number of neurons needed for each hidden layer, though this could be linked to the reason why it can easily generalize. A very important feature also of this neural network is its parallel computing character. This makes it able to produce an output corresponding to its input even though the network had no prior knowledge of it during training. The basic algorithm is the back-error-propagation algorithm in which weights of the neuron are altered in iterative steps to limit the error between the measured and desired output. Such a process is termed 'supervised learning'.

3.2 The neuron model

A neuron can be expressed as a function that computes the output in relation to the input. The main idea of this model is the activation function being adopted. Figure 3.2 shows the basic model of a neuron.

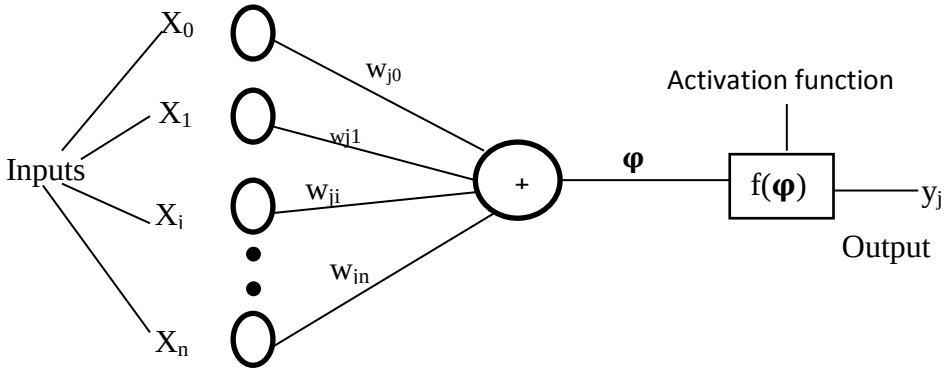

Figure 3.2: Basic Neuron Model

$$y = f(\varphi) = f\left(\sum_{i=0}^{n} w_{ji}\ x_i\right) \tag{3.1}$$

Where y is the output of the neuron, $f(\varphi)$ is the activation function of the neuron, φ is the summation output signal

$$\varphi = W^T X \tag{3.2}$$

and

$$W = [w_0, w_1 \ldots . w_{jn}] \ , \ A = [X_0, X_1, \ldots X_n]^T \tag{3.3}$$

The change weight Δw_{ji}, weight of a connection between neurons i and j is given as

$$\Delta w_{ij} = \eta \delta_j x_i \tag{3.4}$$

Where;

η : Learning rate

δ_j : Change rate and depends on if neuron j is an output or hidden neuron

For output neuron;

$$\delta_j = (\partial f / \partial net_j)(y_{jt} - y_j) \quad (3.5)$$

and for hidden neurons;

$$\delta_j = (\partial f / \partial net_j)(\sum_q w_{jq}\, \delta_q) \quad (3.6)$$

where;

net_j : Total weighted sum of input signals to neurons j

y_{jt} : Target output for neuron j

δ_q : change rate for hidden neuron

In-order to speed up the training process, momentum constant (μ) is added and the equation given as

$$\Delta w_{ij}(I + 1) = \eta \delta_j x_i + \mu \Delta w_{ij}(I) \quad (3.7)$$

Where;

$\Delta w_{ij}(I + 1)$: weight change in epochs (I+1)

$\mu \Delta w_{ij}(I)$: weight change in epoch (I)

The activation function decides what power the output from the neuron would be depending on the sum of its inputs. Different activation functions are known and its application depends on its use. The function could be Linear, hyperbolic tangent sigmoid, logistic sigmoid or Gaussian RBF. This difference is as shown,

- Linear

$$F(x) = x$$

- Hyperbolic Tangent sigmoid

$$F(x) = \frac{e^x - e^{-x}}{e^x + e^{-x}}$$

- Logistic sigmoid

$$F(x) = \frac{1}{1+e^{-x}}$$

- Gaussian RBF

$$\boldsymbol{\varphi}_j(x) = \exp\left(-\frac{1}{2\sigma_j^2}\left\|x - x_j\right\|^2\right)$$

Depending on the interconnection of the neurons in a model, neural networks can be broadly divided into two main types. They are the feed-forward and the recurrent or feedback network. For the feedback network, circlets exist in the network connection, thus there is a feedback into the network along with its inputs. Owing to the simple nature and a well analyzed algorithm, the feed forward network is mostly used and has also been applied in this thesis work.

3.3 Feedforward Networks

These are the simplest types of network. It is devoid of loops or feedback connections thus its information travel in a unidirectional form. In the family of feedforward network, the most commonly applied is the layered network were neurons are structured into layers with its links emanating precisely from one direction from one layer to the next.

3.4 Learning Method

The main idea behind neural network successful application in various fields is to know the weight to realize the desired target and that process is described as training or learning. Two different learning methods are often been used; supervised learning and the unsupervised learning. Supervised learning modifies the weight with the objective of minimizing the errors between the given input set and target set [17]. Thus, in this mode, the input data and the corresponding target that should exit from

the network are known. Hence neural network is aware of both the inputs and target values. For the unsupervised learning, the data set used in training the data has only a known input value. Thus, it is pertinent to choose the right set of examples for training to achieve an efficient training. The Self-Organizing Map and the Adaptive Resonance Theory algorithm are the most commonly used unsupervised learning algorithms. The structure of the network determines the learning strategy to be used. For a feedforward network, the supervised learning strategy is adopted. It must be noted that the learning process aims at minimizing the error function.

Most often, the activation constant used, is non-linear; thus minimization requires a nonlinear function to handle it, and this nonlinear function adopts the steepest-decent algorithm. From [18], the steepest decent is an addition to Laplace's method for integral approximation. In Levenberg-Marquardt algorithm back error propagation is used [18].

3.3.1 The back-error propagation

This is one of the easiest networks to understand. Learning and update procedure is intuitively appealing because it is based on a relatively simple concept; if the network gives the wrong answer, then the weights are corrected so that the error is lessoned as a result, future response of the network are more likely to be correct. The network is fully layered. Each of the layers is fully connected to the layers below and above. When the network is given an input, the updating of the activation value propagates forward from the input layer of processing units through each internal layer to the output layer of the processing unit and the output unit then provides the network response [19]. Once these internal parameters are corrected, the correction mechanism starts with the output units and propagates backward through each

internal layer to the input layer, hence the word 'back-error-propagation'. Figure 3.4 shows the basic back-error-propagating processing unit.

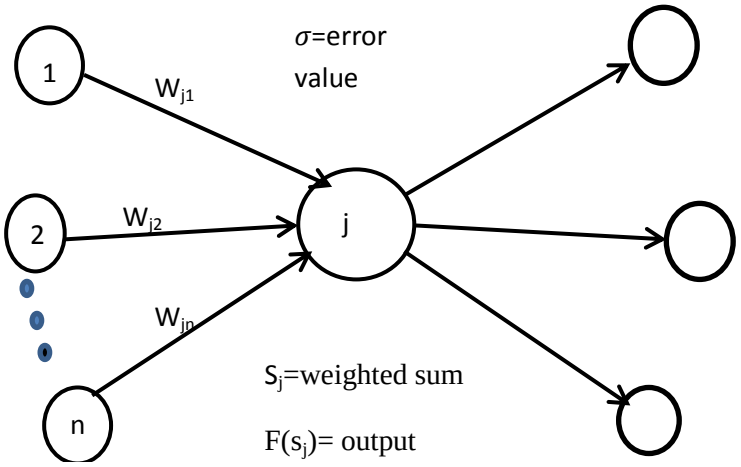

Figure 3.3: Back-error-propagating processing unit

The inputs are at the left and output at the right which receive output from the processing unit at the center. The processing unit has a weighted sum (s_j), an output value a_j and an associated error value (σ_j) applied during weight adjustment. It involves a forward propagating step followed by a backward propagating step. Both forward and backward are done for each pattern presentation during training.

In each successive layer, every processing unit sums its input and then applies a sigmoid function $F(x) = \frac{1}{1+e^{-x}}$ to compute its output.

3.3.1.1 Forward propagation

This gets initiated when an input pattern is presented to the network. Figure 3.5 illustrates this forward propagation;

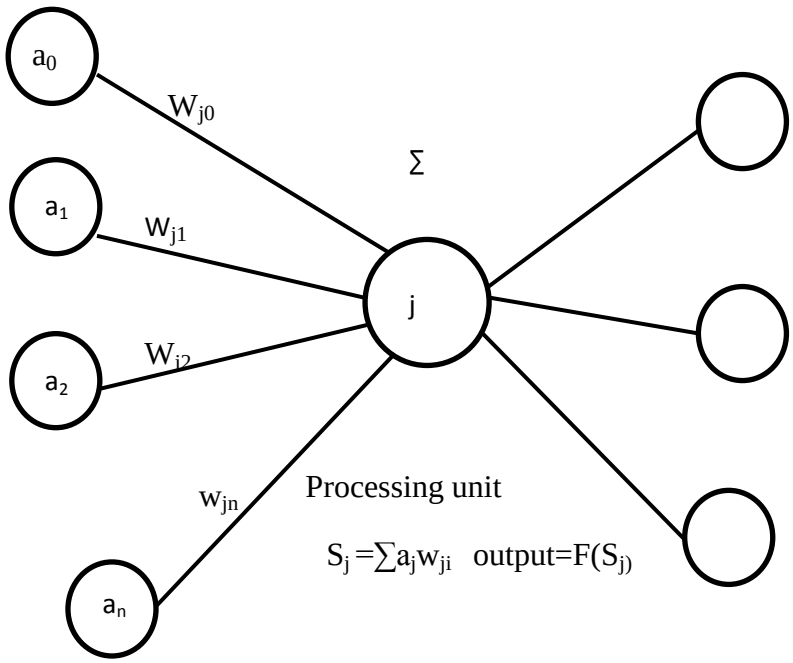

Figure 3.4: Forward processing unit

After setting the activation level for first layer of units, the other layer carries out a forward propagation step which decides the activation layer of other unit layers. Incoming connections to unit j are at the left and originates at unit below, not shown here. The outputs are summed up using

$$S_j=\sum_i a_i\, w_{ji} \tag{3.7}$$

After S_j function [f] is used to compute S_j and f is the sigmoid function.

3.3.1.2 Backward Propagation

Here, the error values are calculated for all processing units and weight changes are calculated for all interconnections. It begins at the output layer and moves via the network to the input layer. The error value (σ) is used to compute for the output layer and is somewhat more complicated in the hidden layer [20]

For instance, if unit j is in the output layer,

$$\sigma_j= (t_j-a_j)\, f'(S_j) \tag{3.8}$$

where;

t_j = target value for unit j

a_j = output value for unit j

$f'(x)$ = derivative of sigmoid function f

S_j = weighted sum of input to j

$(t_j - a_j)$ = amount of error

Figure 3.6 shows the processing unit in a hidden layer.

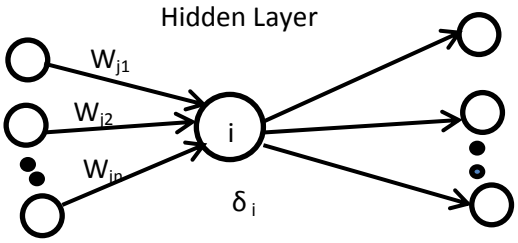

Figure 3.5: Processing unit in hidden layer

Chapter 4

METHODOLOGY

4.1 Insulator contour optimization

The electrical field distribution and the tangential stress on the surface of an electrode and insulator should be uniformly distributed in order to reduce the effect of flashover, partial discharge and even puncture. The main objective of the optimization process is to ensure uniform and minimal electric filed stress on the surface of the insulator.

Partial discharge usually starts from areas with uneven distribution and gradually proceeds to areas evenly distributed. Continuous discharge could lead to a puncture of the insulating media and may lead to a breakdown of the entire system. The shape of the insulator used in high voltage transmission should be taking into cognizance as it is one of the main determining factors influencing electric field distribution [21], thus to have an insulator with minimal electric field and uniformly distributed stress, its surface geometry must be smoothened as possible. For instance, the widely used commercial pin insulator is seen to have irregular surface especially along its shed. This irregular surface increases the electric field stress in concentrated parts of its geometry.

For improved efficiency, increased life span of power system, the insulator employed must be well optimized. In this study, a commercial pin insulator used for high voltage transmission is optimized using neural network. The network is trained with

the geometry and electric field obtained from its surface and the contour of the insulator found optimal and thus obtaining an even electric field distribution.

4.2 Data collection methods

Various techniques are deployed when collecting data. These techniques are grouped into six types [22]. These include Interviews, questionnaires and surveys, observation, focus groups, ethnographies, documents and records. For the purpose of this research work, the observation method was applied**.** The observation method, allows one to study the dynamic of the situation under view, frequency counts of target behavior and acts as a good source of providing qualitative and quantitative data.

4.2.1 Data collection using Observation method

For this research work, a 2D axisymmetric pin insulator as shown in Figure 4.1 is used. R_1, R_2, R_3, and R_4 are varied at different times in order to obtain different insulator profiles. In the first case, the R_1 curvature was varied from a radius of 1.0 cm to 1.5 cm at a step of 0.01 cm while R_2, R_3, R_4 held constant at a value of 0.5 cm. This generated 51 different patterns. On the other case, R_1 held constant at a value of 1.5cm while varying R_2, R_3 and R_4 from a radius of 0.5 cm to 1.5 cm at a step of 0.02 cm. This also yields another 51 patterns of the geometry. In total, 102 patterns are obtained. The height (H) of the insulator kept fixed at 18.9 cm and R_5 kept fixed at 0.5cm.

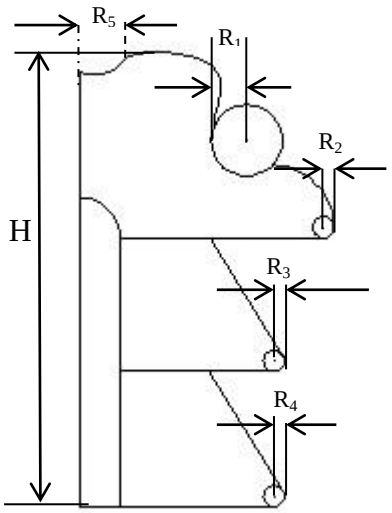

Figure 4.1: 2D view of the pin insulator

Then, the finite element method is applied to calculate electric field intensities with help of the finite element software 'COMSOL'. This first discretize the domain into a finite number of elements in the form of mesh, Figure 4.1. The live conductor with a voltage of 1kV is supported at R_5. This applies the electric field experienced on the insulator. Relative permittivity of the insulator taken to be 5 since a porcelain material is used and that of the surrounding environment placed at 1 (relative permittivity of air). Part of the insulator that is connected to the tower is grounded. The mesh is physics controlled and an element size of finer (simple tiny triangular nodes) adopted in order to have a more accurate result. It is pertinent to note that, the smaller the mesh sizes, the more accurate the results are likely to be. The equipotential distribution of the insulator is shown in Figure 4.2.

Finally, the maximum line electric field along the tangential component of the insulator contour, its surface average and the surface maximum are collected.

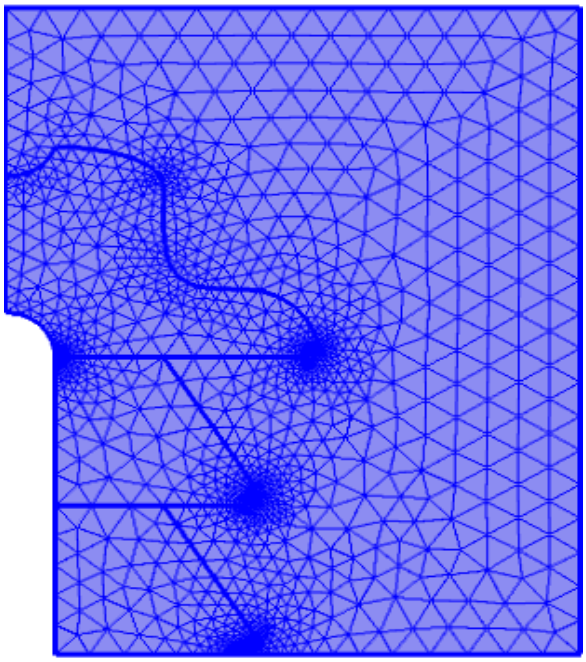

Figure 4.2: Triangular meshing

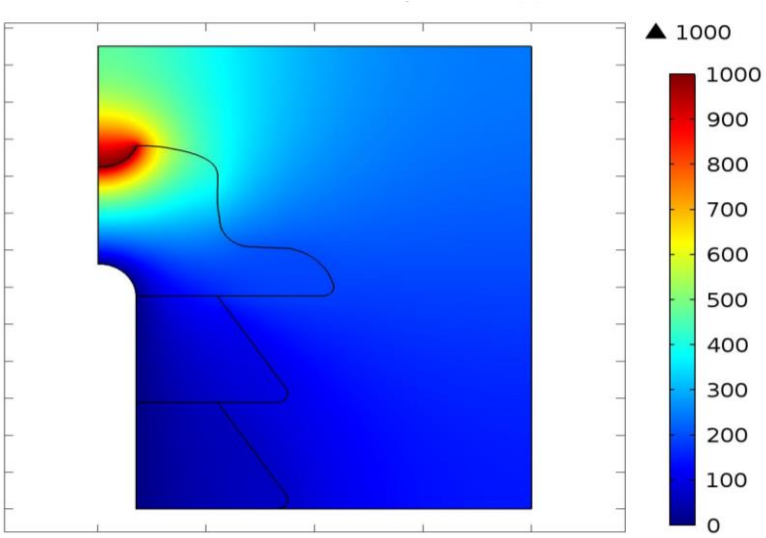

Figure 4.3: Surface Electric Potential

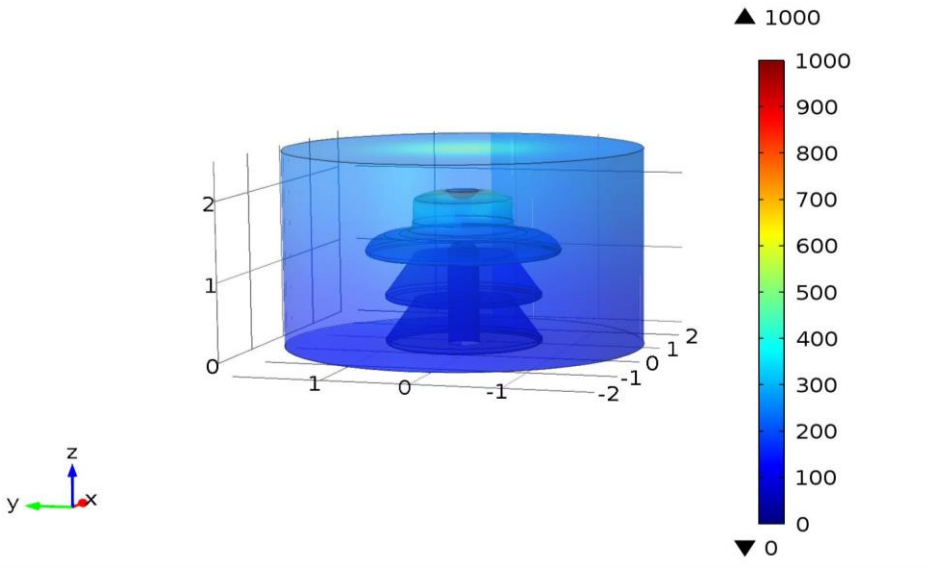

Figure 4.4: 3D view of the surface electric potential

At the end of this process, the inputs and target parameters required for the neural network training and testing are obtained. Its input are the different electric field collected (maximum line electric field, maximum surface electric field and the surface average electric field) and the target are the geometrical coordinates (R_1, R_2, R_3 and R_4).

4.3 Designing the Artificial Neural Network

4.3.1 Data Normalization

After the data has been collected using the observation method by applying the finite element method with the help of COMSOL, as described in 4.2, the data are imputed into the neural network. In the network, the data is first normalized since it has varying ranges in its data. Tymvios et al. [23] 'states that mixing variables with large magnitude and small magnitude confuses the learning algorithm and could force it rejecting the variable with lesser magnitude.

4.3.2 Network building

The multilayer perceptron network is used for this research work. The training algorithm selected for this work is the Levenberg-Marquardt. Number of inputs specified to be three while its output specified four, other network parameters used includes; one hidden layer and the number of neurons ten. The epoch which is otherwise described as the training cycle is fixed at 1000, built in transfer function provided by Matlab used for this work is the logistic sigmoid.

$$f_{(x)} = \frac{1}{1 + e^{-x}} \tag{4.1}$$

4.3.2.1 Learning rate (η)

Success and conjunction of the algorithm depends largely on this parameter. It is recommended that a small value of learning rate be used. It must be noted that every system has its own learning rate.

4.3.2.2 Momentum constant (μ)

This helps in preventing the system from converging to a local minimum. It's also useful in helping to speed up the system convergence.

4.3.2.3 Hidden neurons

They are neither in the output nor input layers. In fact, they are hidden from view. The number of neurons in a system affects the complexity of the algorithm and processing power. High number of neurons increases the complexity of the algorithm but increases its processing power. Very few numbers of hidden neurons leads to the system taking longer training period [24].

4.3.3 Network training

In this process, the neural networks learn from the inputs and update itself accordingly with reference to varying weight. Thus sets of data are required for this feat. The data imputed into the network has both an input and a target, thus the

network has an idea of what the output looks like. Slowly, the network learns from the data imputed and gradually develops the ability to generalize and eventually produce an output when new data are introduced.

For the training of this network, the normalized data is used. The electric field is specified as its input data while the different curvature radii are taking as its target. The leaning rate (η) and the momentum ($\boldsymbol{\mu}$) constant is varied between 0.1 and 0.9. For instance, at lr= 0.1, mu varied from 0.9 to 0.1 at a step of 0.1. This process is repeated for values of lr from 0.1 through 0.9 at steps of 0.1 as well. Different numbers of neurons have been considered as well.

4.3.4 Network Testing

Having finished training the network, the next step is testing. Testing helps check the generalization performance for the network. Various ways are employed in testing the network. In this work, a statistical method is applied to quantitatively analyze the system, and to ascertain the error in both training and testing. These are the root mean square error (RMSE) and the maximum absolute error (MAE). The MAE is a measure of the average magnitude of errors in a set of forecast and it is a linear score; meaning all individual differences is weighted equally on the average. The RMSE is used when large errors are undesirable and usually higher than the MAE or equal. When RMSE equals MAE, it means all errors are of same magnitude. RMSE represent the error in training while the MAE represents error for testing. Equation (4.2) and (4.3) shows the formula for both RMSE and MAE respectively.

$$\mathrm{RMSE} = \sqrt{\frac{1}{M_P\, M_k}\sum_{P=1}^{M_P}\sum_{K=1}^{M_K}(t_{PK} - O_{PK})^2} \tag{4.2}$$

$$\mathrm{MAE} = \frac{1}{M_N M_K} \sum_{P=1}^{M_N} \sum_{K=1}^{M_K} \left[\frac{|t_{PK} - O_{PK}|}{t_{PK}} \right] 100 \tag{4.3}$$

Where, t_{PK} = measured value, O_{PK} = Network predicted value, M_N= number of test cases.

The flow chat for developing the MLP network in Matlab is shown in figure 4.5

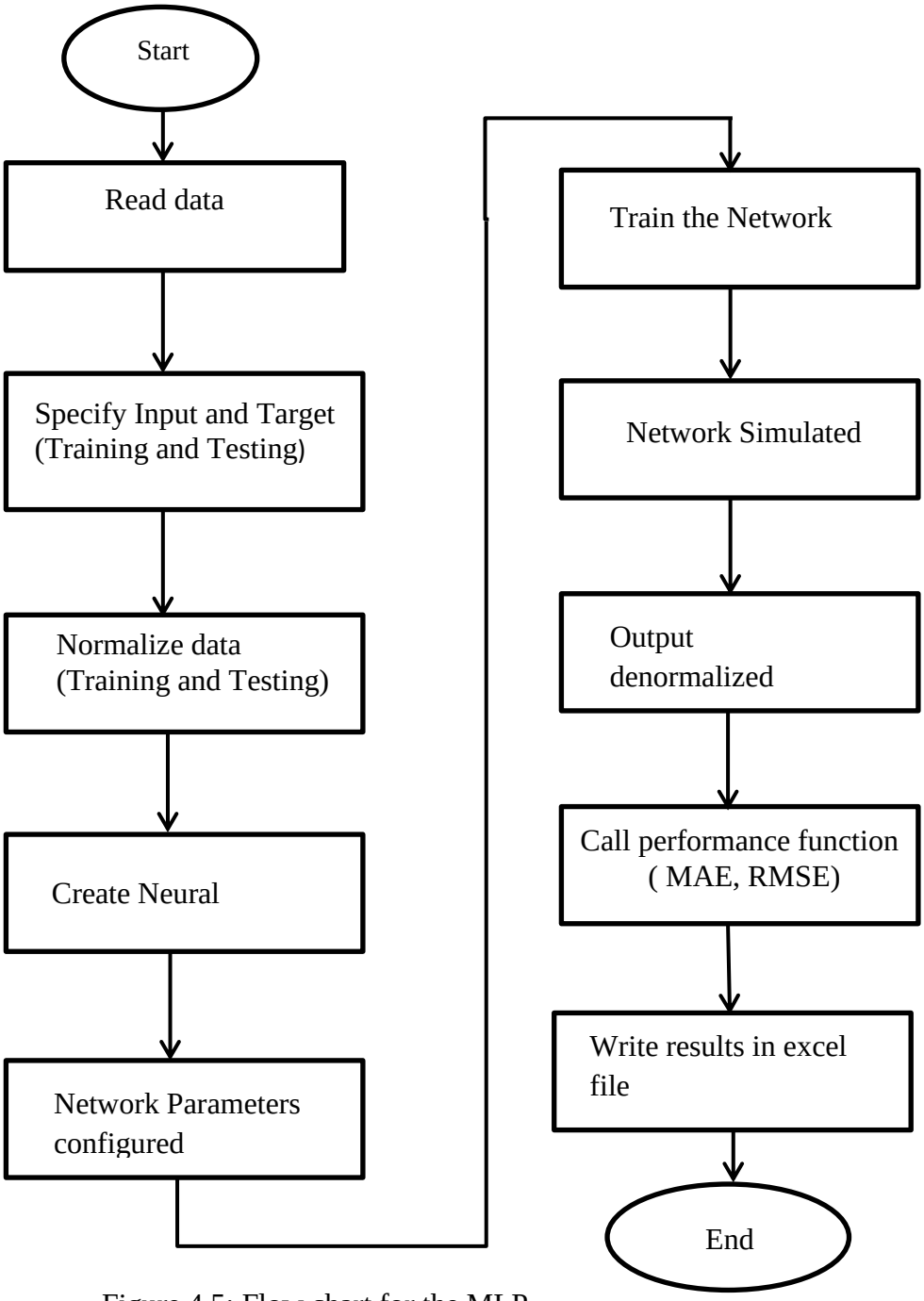

Figure 4.5: Flow chart for the MLP

Chapter 5

RESULTS AND DISCUSSION

The flow chart of Figure 4.5 with respect to the methodology shows the different steps taking in training the network. This training is implemented using the Matlab software. The mean absolute error (MAE) for testing and the root mean square error for training are obtained respectively using different learning rate, momentum constant and different number of neurons. Though both RMSE and MAE are used for the error correlation in the network, for the purpose of this optimization process, more attention is paid to the MAE of the test cases.

5.1 Effect of momentum constant (μ)

The momentum constant helps to prevent the network from converging at a local minimum. It is varied from 0.1 through 0.9 at step of 0.1. The result obtained is shown in Table 5.1 and Figure 5.1.

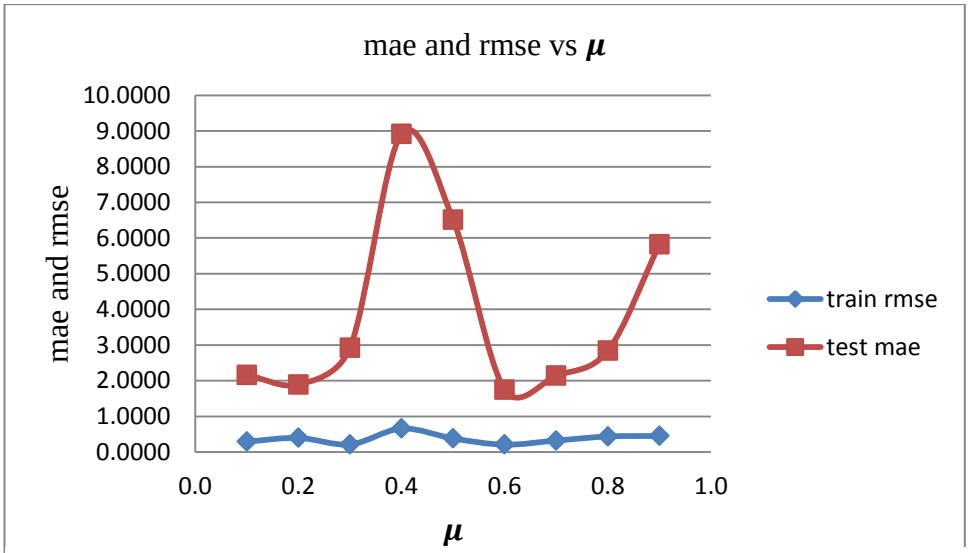

Figure 5.1: MAE and RMSE for varied momentum constant (μ)

Table 5.1: MAE and RMSE for varied momentum constant (μ).

		effect of the momentum constant			
		train		test	
	η=0,1	RMSE	MAE	RMSE	MAE
μ	0.9	0.4514	0.3248	12.9015	5.8202
	0.8	0.4365	0.4360	5.2112	2.8424
	0.7	0.3224	0.2145	5.1007	2.1415
	0.6	**0.2077**	**0.3221**	**3.0842**	**1.7474**
	0.5	0.3802	0.2881	15.6999	6.5079
	0.4	0.6579	0.6744	22.2838	8.9187
	0.3	0.2146	0.1919	7.2824	2.9224
	0.2	0.3962	0.2238	2.9476	1.8938
	0.1	0.2931	0.2466	6.2718	2.1629

From Figure 5.1 and table 5.1, it is observed that the MAE and RMSE have its lowest value at a momentum constant of 0.6. This indicates that this momentum constant has the optimum accuracy since it has the lowest values. It is also seen that there is closeness between the MAE and the RMSE at 0.6 which indicates the closeness of variance in the errors. Therefore, 0.6 is chosen.

5.2 Effect of learning rate (η)

The learning rate is varied between 0.1 through 0.9 at a step of 0.1. The results of the MAE and RMSE obtained are shown in Table 5.2 and Figure 5.2

Table 5.2: MAE and RMSE for varied learning rate

		effect of the learning rate			
		train		test	
	μ=0.1	rmse	mae	rmse	mae
η	0.1	0.2931	0.2466	6.2718	2.1629
	0.2	0.3110	0.2888	10.7189	3.5105
	0.3	0.3889	0.2341	13.2886	3.2434
	0.4	**0.2333**	**0.1251**	**2.7754**	**2.1086**
	0.5	0.3114	0.2273	3.4510	2.8979
	0.6	0.5581	0.3488	3.7674	2.7979
	0.7	0.3060	0.2151	2.6179	2.7270
	0.8	0.4952	0.3610	12.5855	6.7775
	0.9	0.4852	0.304	8.0596	2.62

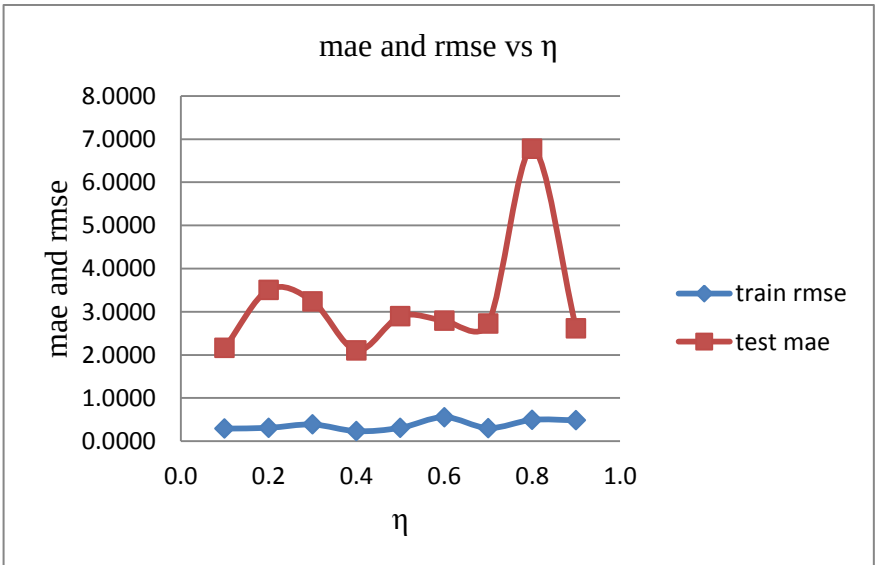

Figure 5.2: MAE and RMSE for varied learning rate (η)

With the varying learning rate, Table 5.2 and Figure 5.2 show the best value at 0.4 since it has the least error rate. Thus the optimized value required lies within the learning rate value and is chosen.

5.3 Effect of number of neurons in hidden layer

Different numbers of neurons are considered to know the best value that produces the least error in the network. Table 5.3 shows the different neurons used and the corresponding MAE and RMSE obtained.

Table 5.3: MAE and RMSE for varied number of neurons

		effect of the number of neurons in hidden layer				
		train		test		
# of neurons in hidden layer		rmse	mae	rmse	mae	
	8	0.3514	0.3121	10.5450	4.6147	
	9	0.2873	0.1193	3.5644	2.0450	
	10	**0.2387**	**0.3028**	**2.1810**	**1.0911**	
	11	0.2547	0.1556	3.7983	1.8424	
	12	0.3309	0.2236	10.2201	2.7621	
	13	0.2960	0.1417	16.3997	9.4015	
	14	0.2686	0.1656	9.4162	4.0194	
	15	0.2531	0.1815	5.4975	3.2461	
	16	0.2355	0.1535	12.5766	4.6775	

From Table 5.3, it is seen that MAE and RMSE has the least values when 10 neurons are used in the network. Therefore, this is chosen as the best value for the optimum prediction. Figure 5.3 further shows a graphical picture of this value.

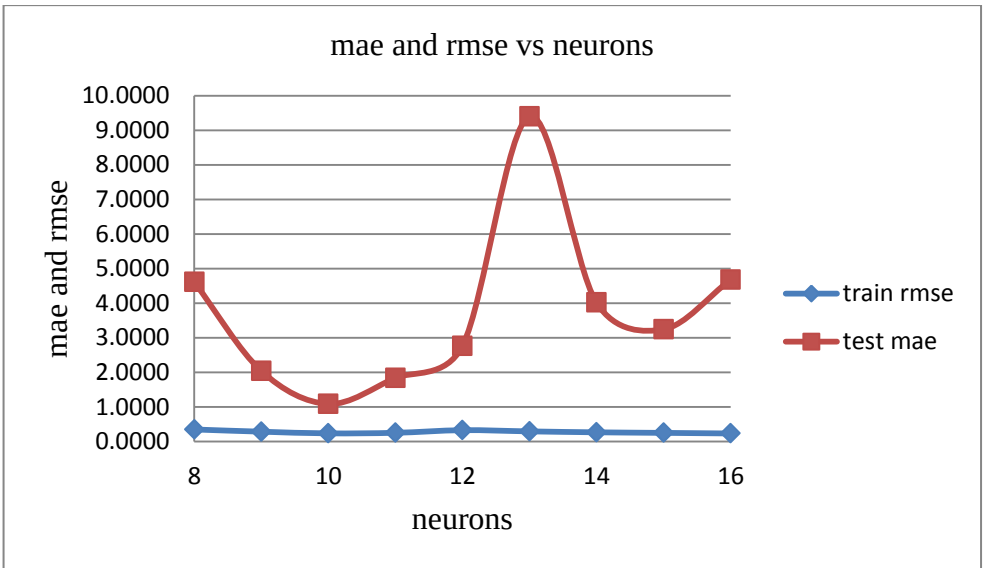

Figure 5.3:MAE and RMSE for varied number of neurons

In order to obtain the best performance for the contour prediction, the optimum values for some variables are used. This variable are 0.1 for learning rate, momentum constant 0.6, number of neurons 10, iterations 1000. These values are obtained from the best performance of the MAE and RMSE. This results in the optimum geometry of the insulator. The performance of the network is shown in the Figure 5.4 by calculating the mean-squared error at each iteration.

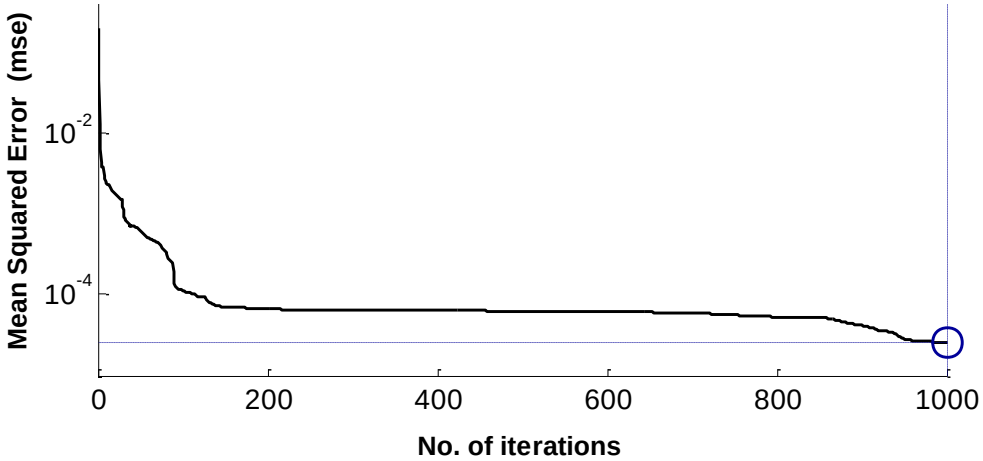

Figure 5.4: Network performance

From Figure 5.4, mean squared error goal set at 0.00001 is achieved at 1000 iterations. This further affirms the network performance.

The optimum contour for the insulator has been determined by using the field distribution. The most uniform and minimum field values are fed to the network to get the optimum geometry. The results for R_1, R_2, R_3 and R_4 are 1.51 cm, 0.4448 cm, 0.4448 cm, and 0.4448 cm respectively. Its electric potential and the arrow surface electric field distribution of the optimized insulator is shown in Figure 5.5.

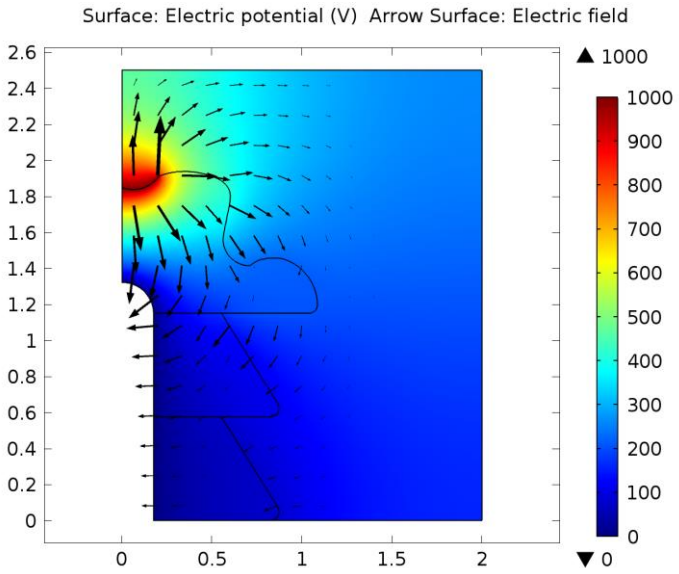

Figure 5.5: Electric potential and Arrow Surface of Electric field

Finally, maximum line electric field along the vertical (z) component of the insulator surface is computed and compared with values of the commercial one and the result is shown in Figure 5.7 and Figure 5.9 respectively. The electric field distribution of both the optimized and commercial insulators is shown in Figure 5.6 and Figure 5.8 respectively.

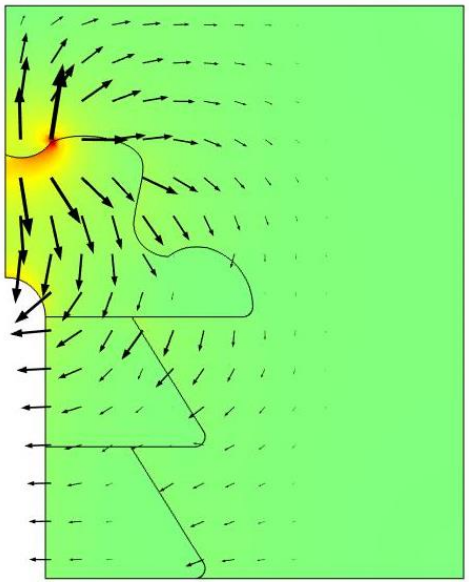

Figure 5.6: 2D Electric field for the optimized insulator

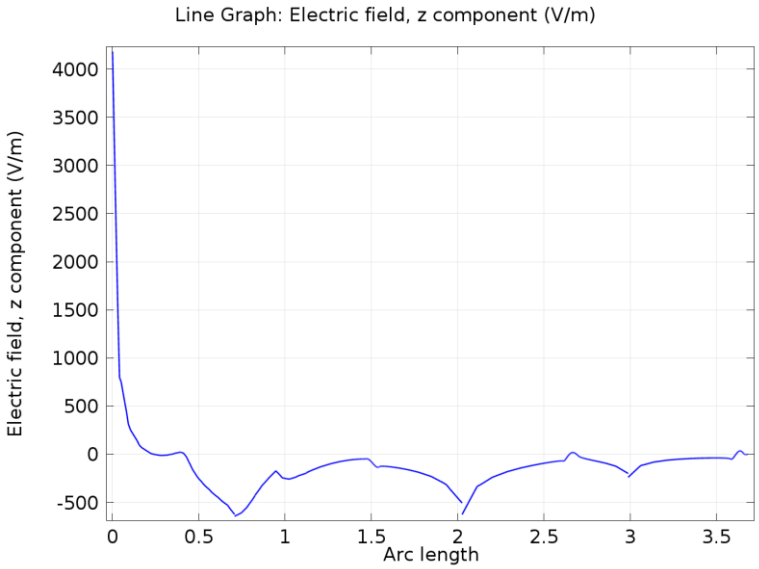

Figure 5.7: Maximum Line component of the Optimized insulator

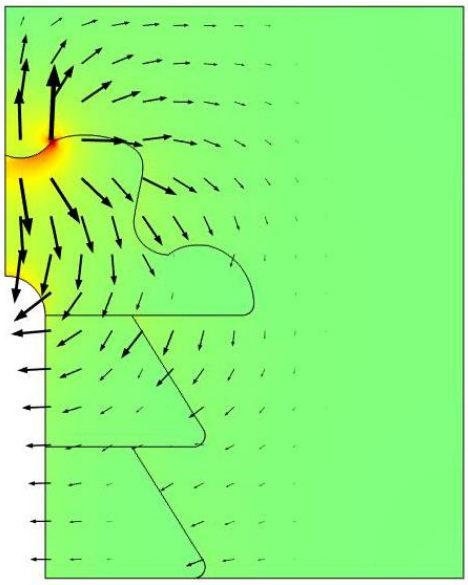

Figure 5.8: 2D Electric field for the commercial insulator

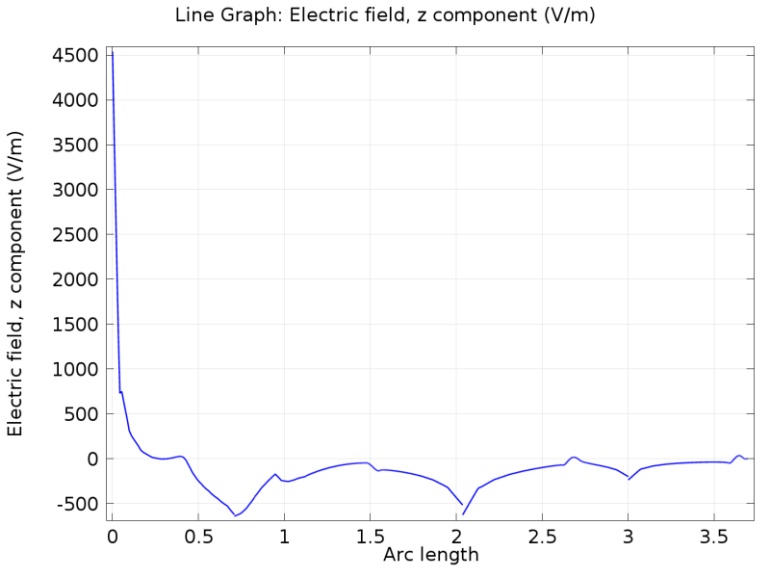

Figure 5.9: Maximum line component of the commercial insulator

From the figures, it is seen that the optimized insulator showed a better performance as compared with the commonly used commercial insulators. This is obvious with Figure 5.9 having higher electric field of about 4500V/m as against Figure 5.7 with 4000V/m.

Chapter 6

CONCLUSION AND FUTURE WORK

6.1 Conclusion

For an efficient and reliable power delivery system, it is of great importance that the insulator employed in the network is well optimized so as to have a minimum but uniformly distributed electric field and tangential stress across it while trying to obtain optimum geometry. In this work, the Artificial Neural Network has been successfully used to optimize the contour geometry of a porcelain pin insulator. With the help of Levenberg-Marquardt learning algorithm, an optimized form of the insulator is achieved. The optimized insulator is compared with the commercial insulators readily used in high voltage transmission and is found to have a better performance as it relates to the desired field distribution. Finally with the help of neural network, a pin insulator is optimized producing an MAE of less than 2% which can be considered as negligible.

6.2 Future Work

For this work, the porcelain pin insulator that is optimized is the ones deployed for high voltage transmission of up to 1 kV. This same model can also be applied to the different types of pin insulators; the material type can be included in the model to enable generalization of the model. In order to increase the network accuracy, dataset should be extended. Different learning algorithms and different network topologies can be applied during training process to investigate their effect on accuracy.

REFERENCES

[1] Banerjee, S., Lahiri, A., & Bhattacharya, K. (2007, April). Optimization of Support Insulators used in HV Systems using Support Vector Machine. IEEE Trans. on Dielectrics and Electrical Insulation, vol. 14(no. 2), pp. 360-367.

[2] Wen-Shiussh, C., Hong-Tzer, Y., & Hong-Yu, H. (2010, July). Contour Optimization of Suspension Insulators using Dinamically Adjustable Genetic Algorithms. IEEE Trans. on Power Delivery, vol. 25(no. 3), pp. 1220-1228.

[3] Phillips, D. B., Olsen, R. G., & Pedro, P. D. (2000, Dec). Corona Onset as a Design Optimization Criterion for High Voltage Hardware. IEEE Trans. on Dielectrics and Electrical Insulation, vol. 7(no. 6), pp. 744-751.

[4] Yundong, C., Xiaming, L., Erzhi, W., Li, J., & Guang, W. (2002, April). Electric Field Optimization Design of a Vacuum Interrupter Based on the Tabu Search Algorithm. IEEE Trans. on Dielectics and Electrical Insulation, vol. 9(no. 2), pp. 169-172.

[5] Kato, K., Han, X., & Okubo, H. (2001). Insulation Optimization by Electrode Contour Modification Based on Breakdown Area/Volume Effect. IEEE Trans. on Dielectrics and Electrical nInsulation, vol. 8(no. 2), pp. 162-167.

[6] Jesus, A. G., & Hermann, S. (1995). Contour Optimization of High Voltage Insulation by Means of Smoothing Cubic Splines. Ninth International Symp. on High

Voltage Engineering,, (pp. pp. 8343-1 -8343-4). Graz Convention Center, Austria, Europe.

[7] Sivathanu, P., Hackam, R., & Alexander, P. H. (1985, Feb.). Influence of Radius of Curvature, Contact Angle and Material of Solid Insulator on the Electric Field in Vacuum (and Gaseous) Gaps. IEEE Trans. on Electrical Insulation, vol. E1-18(no. 1), pp. 11-21.

[8] Bhattacharya, K., Chekravorti, S.,Mukherjee, P.K.(2001). Insulator Contour Optimization by a Neural Network. IEEE Trans. on Dielectrics and Electrical Insulation, vol.8 (no.2) pp.157-161

[9] Chakravorti, S., & Mukherjee, P. K. (1994, April). Application of Artificial Neural Networks for Optimization of Electrode Contour. IEEE Trans. on Dielectrics and Electrical Insulation, vol. 1(no. 2), pp. 254-264.

[10] Maitha, H. A., Assi, A. H., & Hassan, A. H. (n.d.). Retrieved January 10, 2015, from www.intechopen.com

[11] Lam, J., Wan, K., & Liu, Y. (2008). Solar Radiation Modelling using Artificial Neural Network for Different Climate in China. Energy Convertion and Management, vol. 49, pp. 1080-1090.

[12] Maria, M., Marios, A., & Christo, C. D. (2011). Artificial Neural Network for Earthquake Prediction using Time series Magnitude Data or Seismic Electric Signal. Expert Systems with Applications, pp. 15032-15039.

[13] Iwan, N. S., & Owen, T. T. (1990, January). Neural Net Based Real Time Control of Capacitors Installed on Distribution Systems. IEEE Trans. on Power Delivery, vol. 5(no. 1), pp. 266-272.

[14] Kaana, N., Alexander, P. H., & Hackam, R. (1988, April). Potential and Electric Field Distribution at a High Voltage Insulator Shed. IEEE Trans. on Dielectrics and Electrical Insulation, vol. 23(no. 2), pp. 307-318.

[15] Gosh, P. S., Chakravorti, S., & Chatterjee, N. (1995, Dec). Estimation of Time-to-flashover Characteristics of Contaminated Electrolytic Surfaces using a Neural Network. IEEE Trans. on Dielectrics and Electrical Insulation, vol. 2(no. 6), pp. 1064-1074.

[16] Dayhoff, J. E. (1990). Neural Network Architecture. An Introduction. New York: VAN NOSTRAND REINHOLD.

[17] Jayawardena, A., Achela, D., & Fernando, K. (1998). Use of Radial Basis Function Type Artificial Neural Network for Runoff Simulation. Computer Aided Civil and Infrastructure Engineering, vol. 13, pp. 91-99.

[18] Rumelhart, D. E., McClelland, J. L., & PDP Research Group. (1986). Parallel Distributed Processing (Vol. vol. 2). Boston: MIT Press.

[19] Chichoke, A., & Unbehauen, R. (1993). Neural Network for Optimization and Signal Processing. New York: John Wely and Sons Inc.

[20] Haykin, S. (1994). Neural Network. A Comprehensive Foundation. New York: McMillan College Pub. Co. Inc.

[21] Suna, B., & Ozcan, K. (2003). Electrode Contour Optimization by Artificial Neural Network with Levenberg-Marquardt Algorithm. IJCI Proceedings of Intl. XII. Turkish Symposium on Artificial Intelligence and Neural Networks, vol. 1, pp. pp. 1-5.

[22] Minnesota, T. U. (2014). Cyfernet Search. Retrieved February 3, 2015, from www.cyfernetsearch.org/ilm_4_4#observations

[23] Tymvios, F., Michaelides, S., & Skouteli, C. (2008). Estimation of Surface Solar Radiation with Artificial Neural Network in Modelling Solar Radiation at the Earth Surface. Springer, pp. 221-256.

[24] Srivasam, D. A. (1994). Neural Network Short-Term Load Focaster. Electric Power Research, vol. 28, pp. 227-234.